Journal of Geophysical Research: Biogeosciences

Supporting Information for

Estimating the CO_2 fertilization effect on extratropical forest productivity from Flux-tower observations

Chunhui Zhan[1,2], René Orth[1,3], Hui Yang[1], Markus Reichstein[1], Sönke Zaehle[1], Martin G. De Kauwe[4], Anja Rammig[2] and Alexander J. Winkler[1]

[1] Max Planck Institute for Biogeochemistry, 07745 Jena, Germany, [2] School of Life Sciences, Technical University of Munich, 85354 Freising, Germany, [3]Faculty of Environment and Natural Resources, University of Freiburg, 79106 Freiburg, Germany, [4]School of Biological Sciences, University of Bristol, BS8 1TQ Bristol, UK

Contents of this file

Introduction

This supporting information provides 1) the estimation of β and γ effects using different statistical models; 2) tables for information about eddy covariance sites and TRENDY simulations; 3) tests of the statistical method to incorporate the cumulative effect of nitrogen deposition (N_{dep}) to the β estimation.

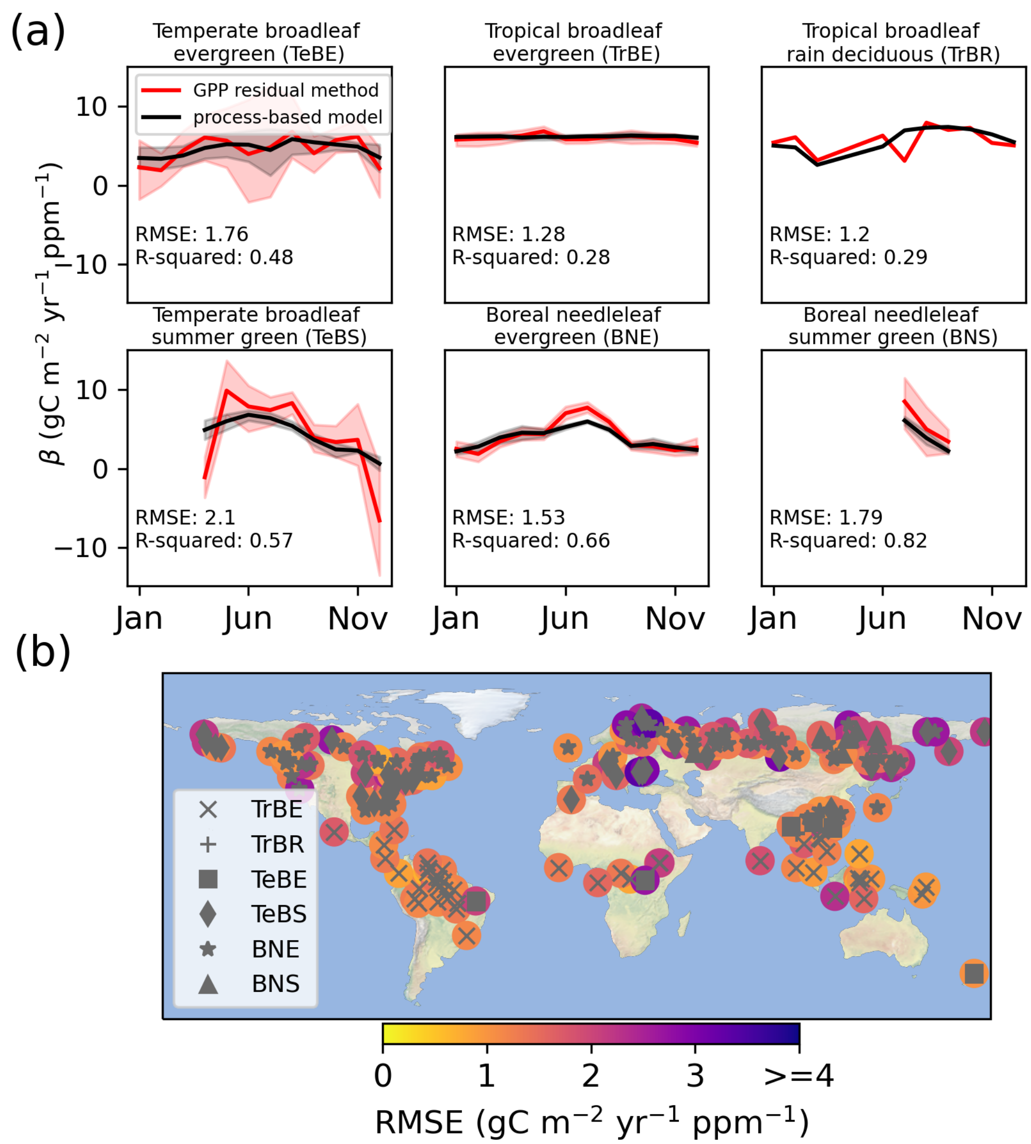

Figure S1. Validation of the statistical method with QUINCY simulations. Analogous to Figure 2 but β is estimated by multivariate regression model.

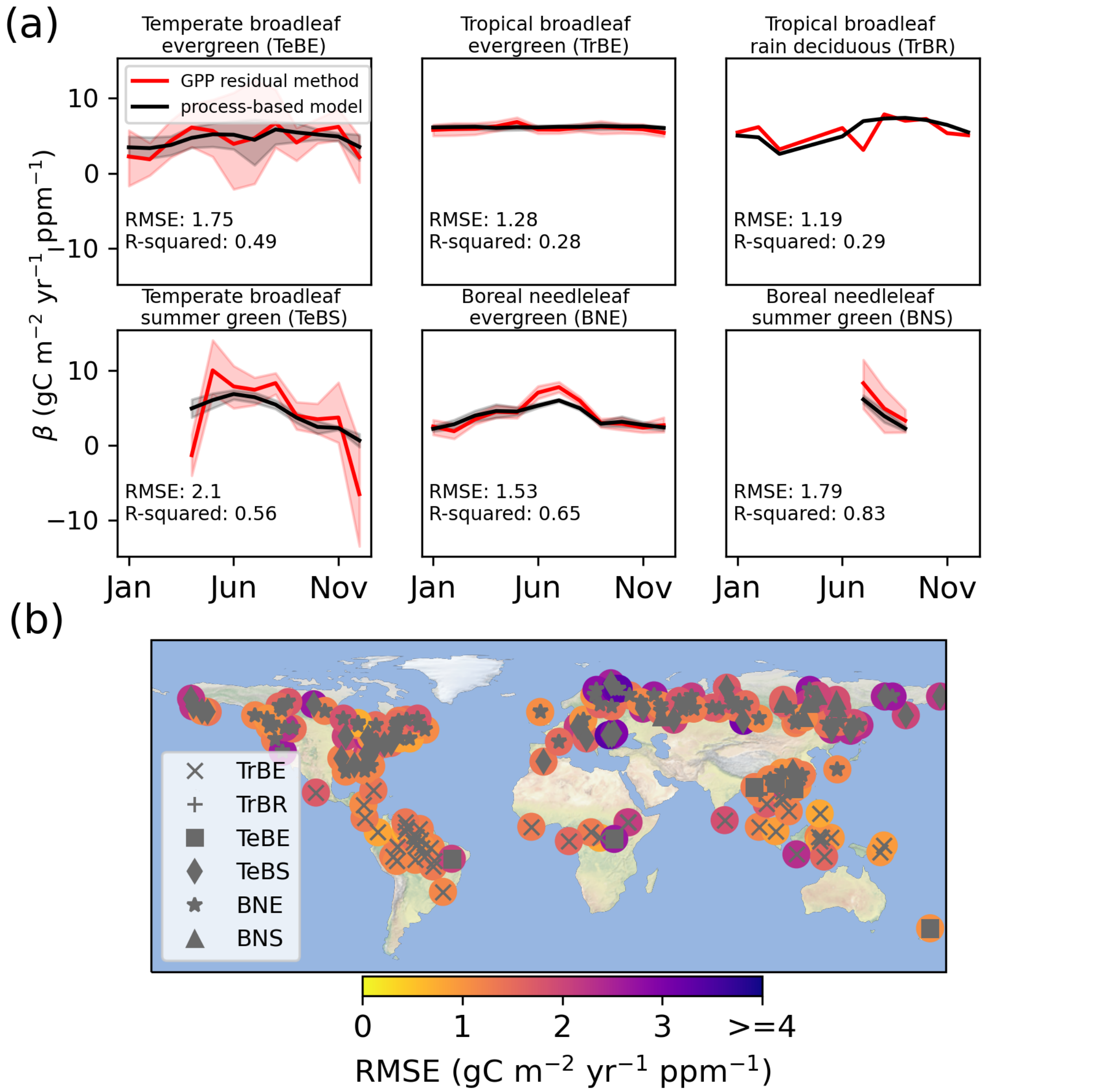

Figure S2. Validation of the statistical method with QUINCY simulations. Analogous to Figure 2 but β is estimated by a simple multivariate regression model.

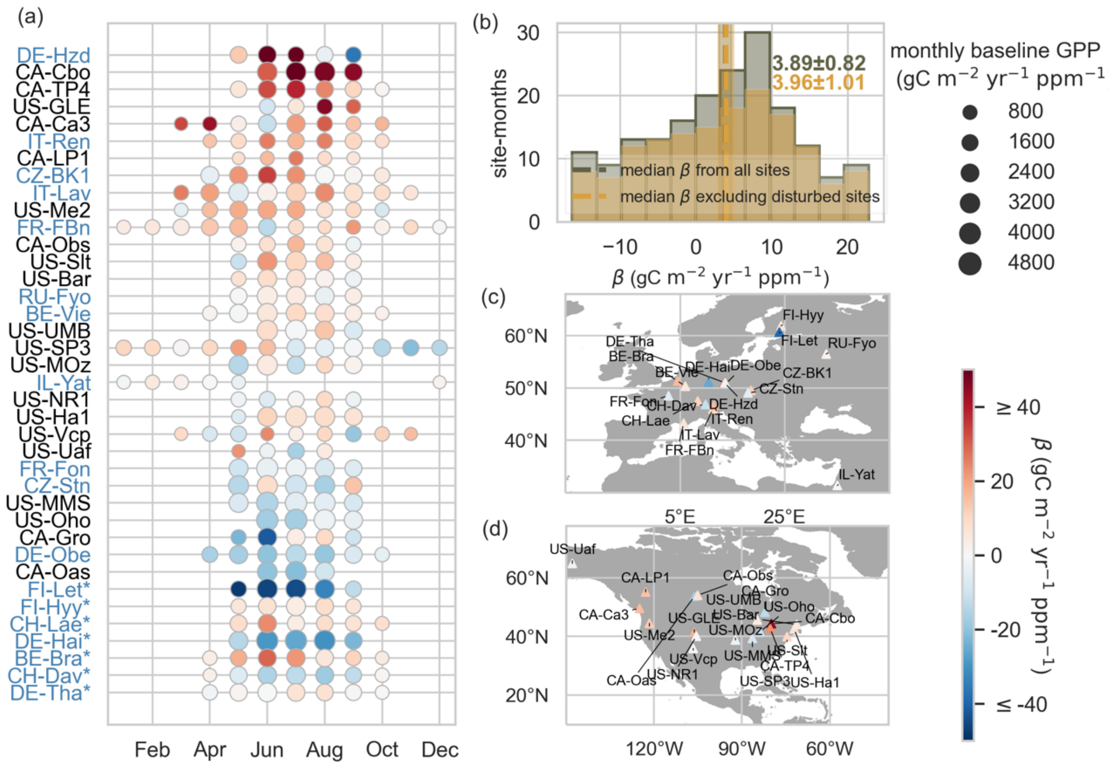

Figure S3. Estimation of β from eddy covariance dataset. Analogous to Figure 3 but nitrogen deposition data from the forcing database for CMIP6 models in included as a predictor of GPP (Methods). Sites in the panel (a) are shown the same order as Figure 3.

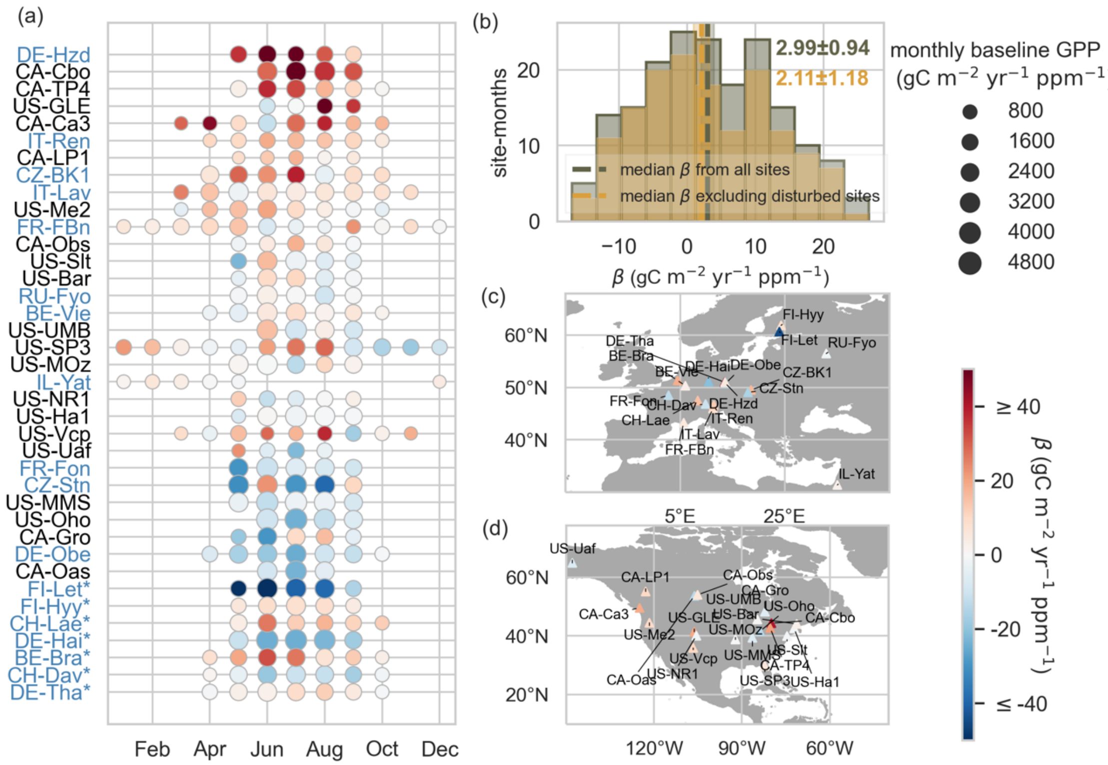

Figure S4. Estimation of β from eddy covariance dataset. Analogous to Figure 3 but β is estimated by a multivariate linear regression model. Sites in the panel (a) are shown the same order as Figure 3.

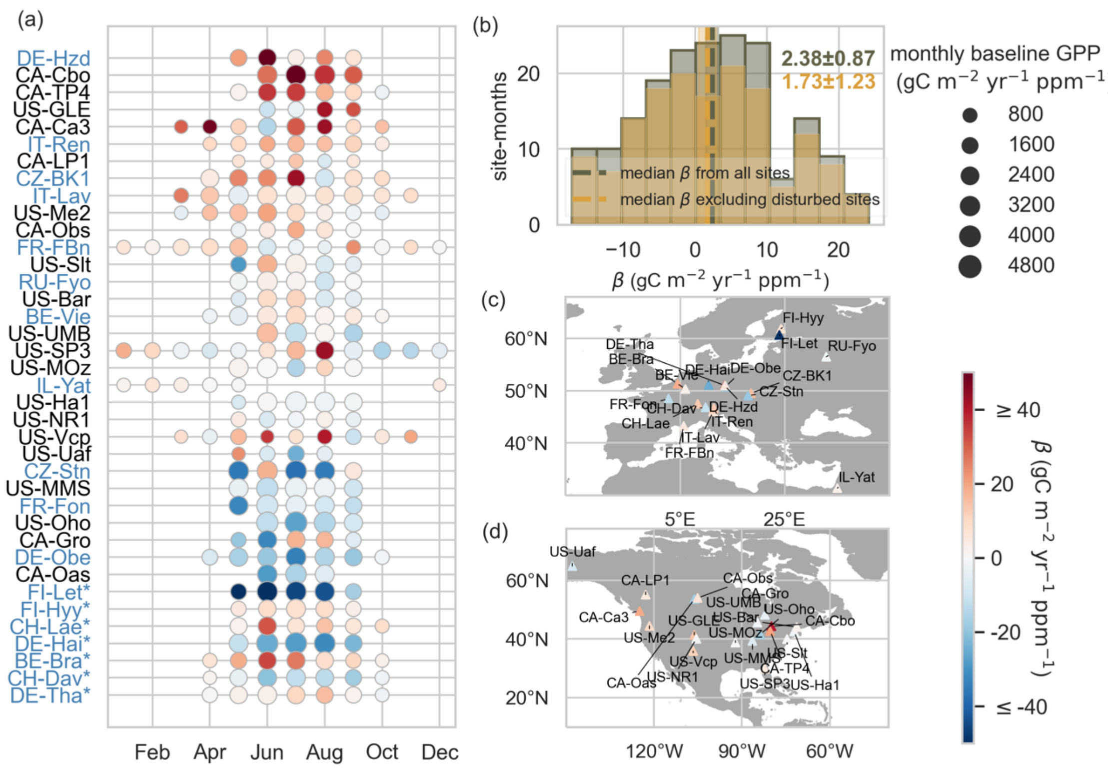

Figure S5. Estimation of β from eddy covariance dataset. Analogous to Figure 3 but β is estimated by the simple multivariate linear regression model (Methods). Sites in the panel (a) are shown the same order as Figure 3.

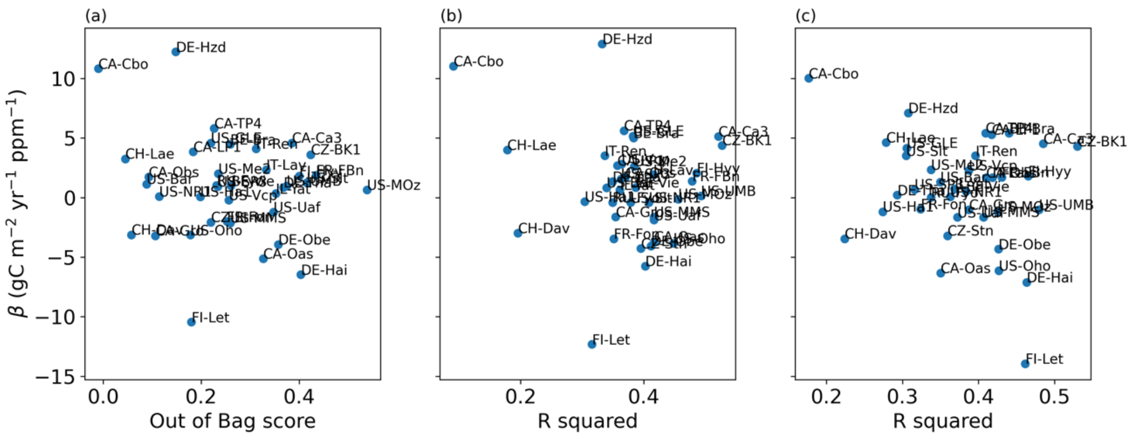

Figure S6. The performance of (a) the random forest model (Out of Bag; OOB score), (b) the multivariate regression model (R squared) and (c) the simple multivariate regression model (R squared) against estimated annual β at each site.

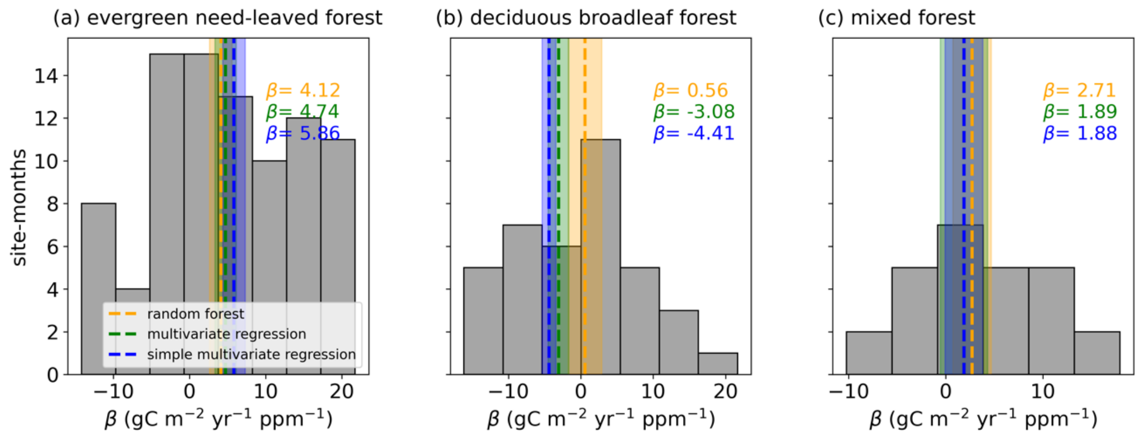

Figure S7. Histogram plots of β estimated for (a) evergreen needleleaf forest (b) deciduous broadleaf forest and (c) mixed forest in eddy covariance dataset. The vertical dashed lines denote the median β estimated from three methods (random forest model in yellow, multivariate regression model in green, simple multivariate regression model in blue). The shaded area indicates the bootstrap estimates for the uncertainty of β correspondingly.

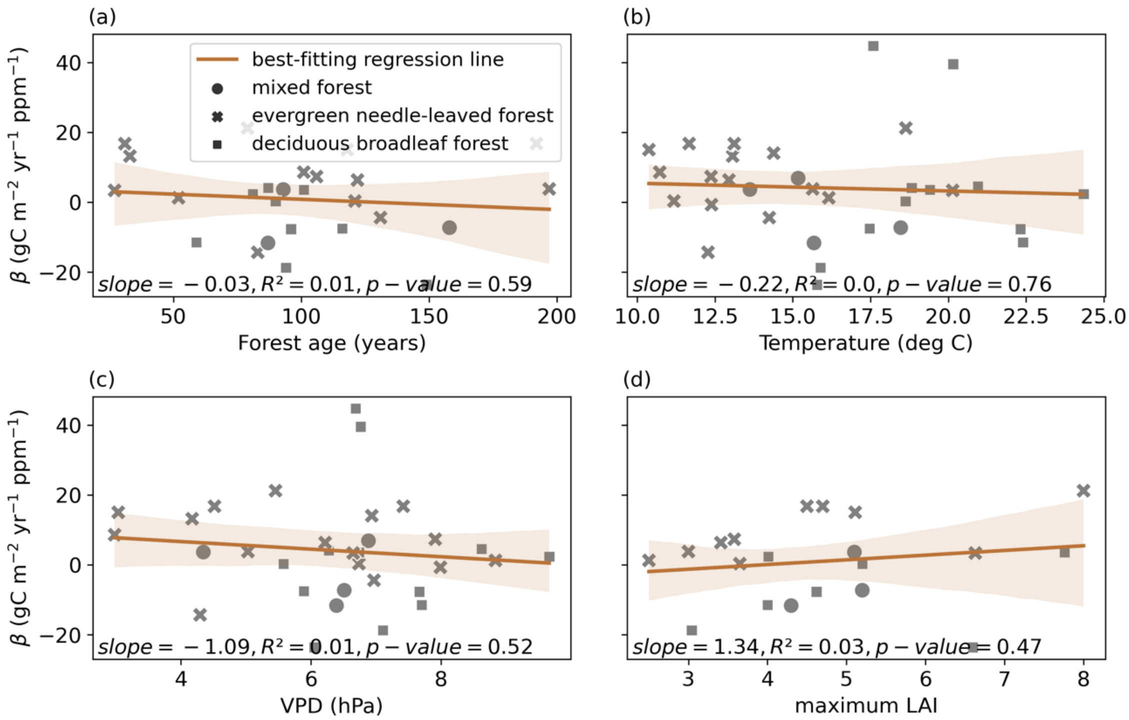

Figure S8. Scatter plot (with best-fitting regression line) and correlation between β and (a) forest age, (b) mean temperature in growing seasons, (c) mean vapor pressure deficit in growing seasons and (d) maximum leaf area index. The shaded area represents the 95% confidence interval around the regression line. Circles, squares and cross represent mixed forest, evergreen needle-leaved forest, deciduous broadleaf forest.

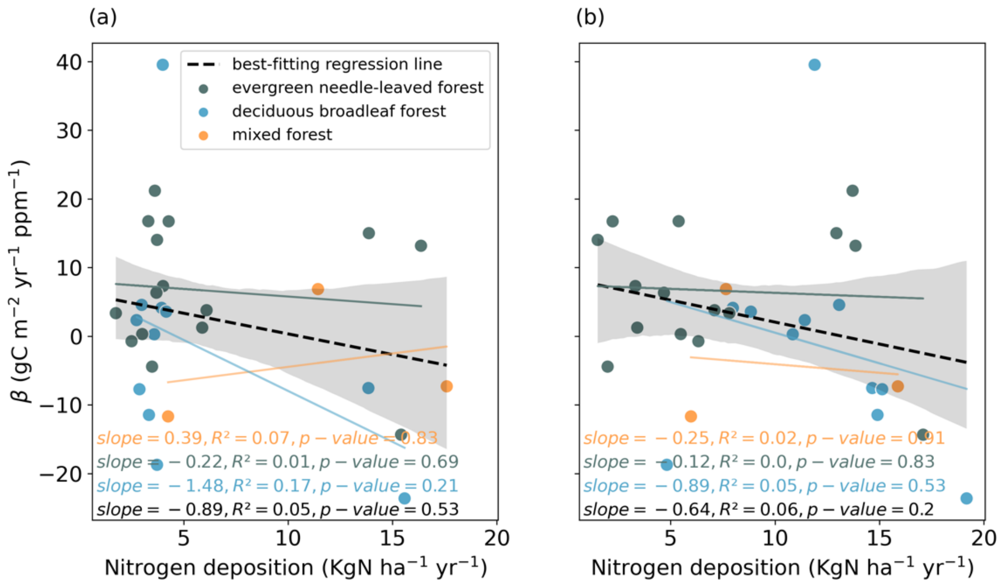

Figure S9. Scatter plot (with best-fitting regression line) and correlation between β and nitrogen deposition data from (a) the European Monitoring and Evaluation Programme (EMEP) Meteorological Synthesizing Centre - West (MSC-W) model, and (b) the forcing database for CMIP6 models. The orange, green, and blue circles represent mixed forest, evergreen needle-leaved forest, and deciduous broadleaf forest, respectively. The best-fitting regression lines for different forest types are depicted in corresponding colors. The shaded area represents the 95% confidence interval around the regression line fitted across all sites.

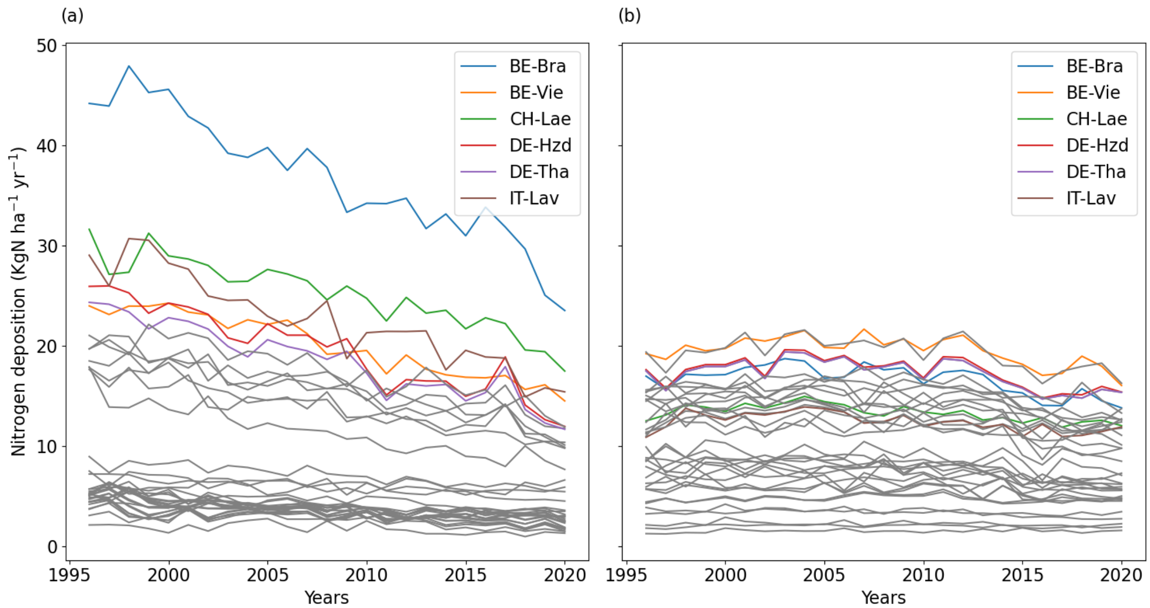

Figure S10. Temporal evolution of Nitrogen deposition (N_{dep}) near the 38 forest sites from 1996 to 2020, using data from (a) the European Monitoring and Evaluation Programme (EMEP) Meteorological Synthesizing Centre - West (MSC-W) model, and (b) the forcing database for CMIP6 models. In instances where the annual N_{dep} remains below 24 KgN ha^{-1} yr^{-1} (Methods) throughout the entire period in panel (a), the lines are depicted in grey. Conversely, when the N_{dep} exceeds this threshold, the lines are presented in different colors. Specifically, N_{dep} data near the sites BE-Bra, BE-Vie, CH-Lai, DE-Hzd, DE-Tha, and IT-Lav are distinguished by unique colors. Although the annual N_{dep} values in panel (b) consistently fall below 24 KgN ha^{-1} yr^{-1}, the color scheme is maintained in panel (a) for consistency.

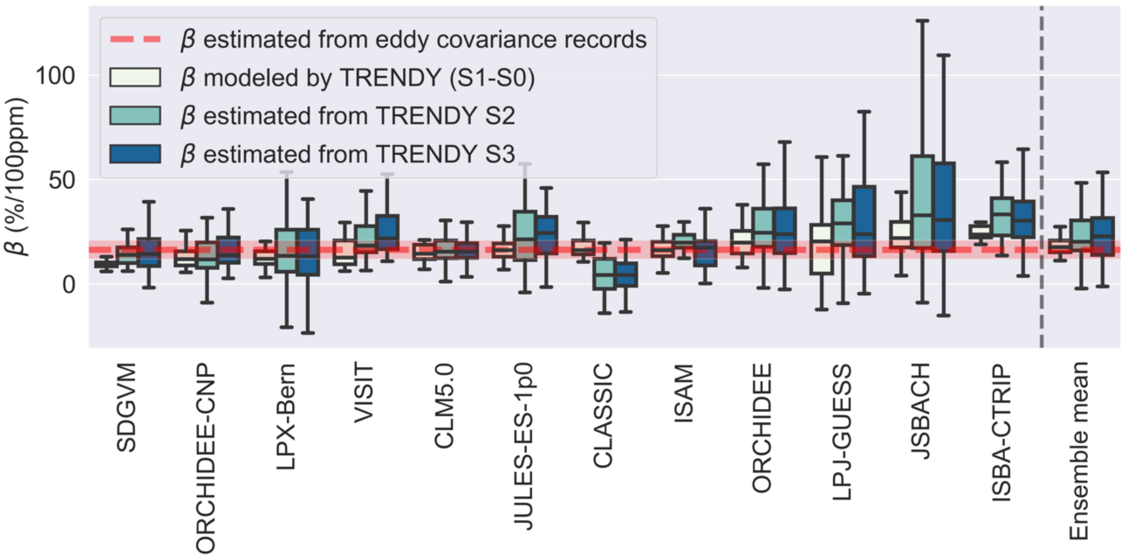

Figure S11. Comparing β estimated from eddy covariance data and the TRENDY model ensemble. Analogous to Figure 5 but β is estimated as the relative change in GPP per 100 ppm increase in atmospheric CO_2 concentration (Methods).

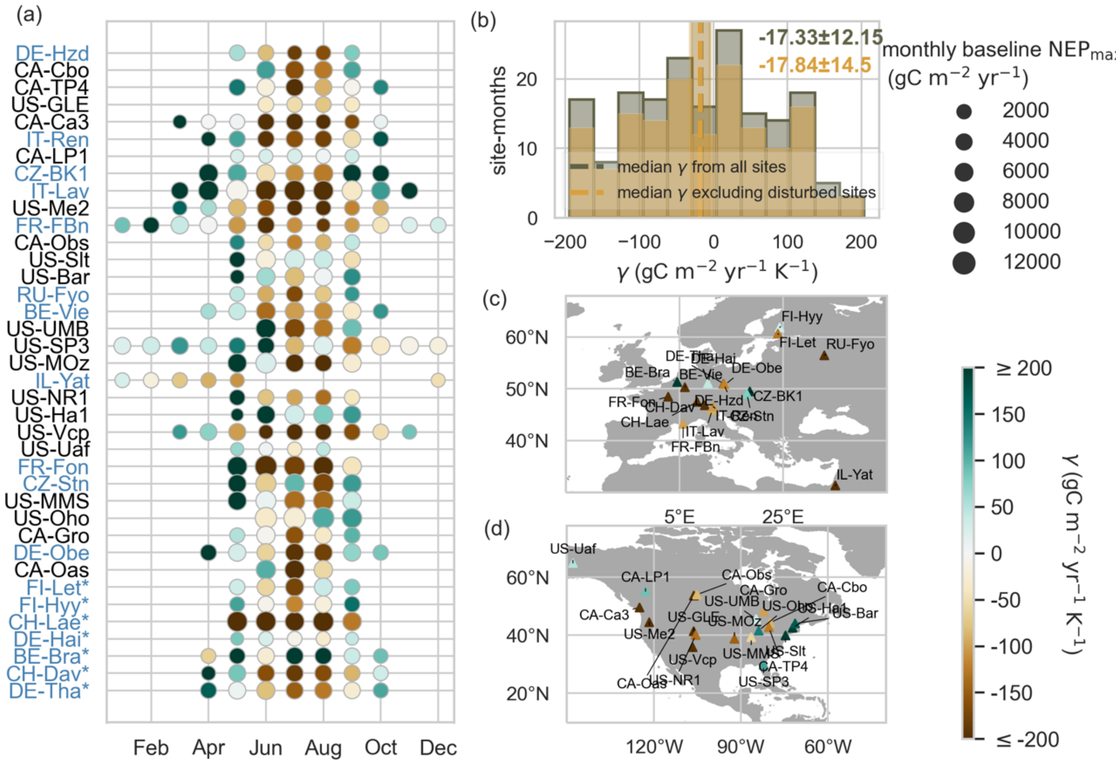

Figure S12. Estimation of γ from eddy covariance dataset using the *GPP residual method* with a random forest model. Analogous to Figure 6 but γ is estimated for NEP_{max}.

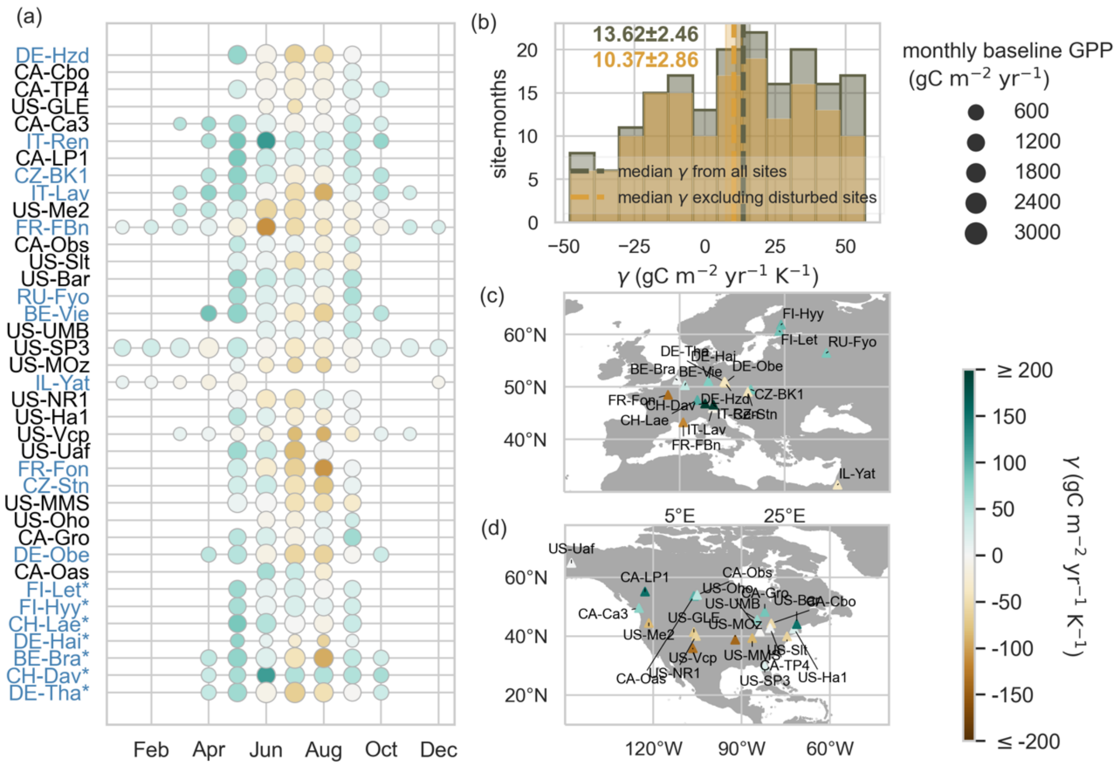

Figure S13. Estimation of γ from TRENDY ensemble mean. Analogous to Figure 6 but γ is estimated from the TRENDY ensemble.

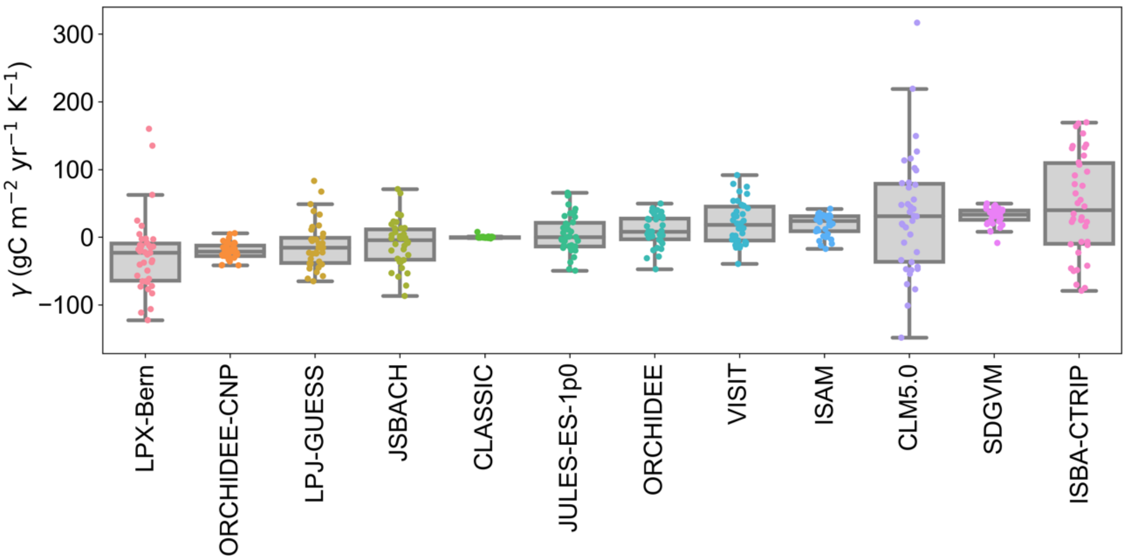

Figure S14. Estimation of γ from the TRENDY ensemble. The medians and interquartile ranges of γ are shown for each model, as horizontal lines within boxes, the upper and bottom lines of the box, respectively. Box plots for individual models are ordered according to the median γ across models. The points represent the mean γ at grid-cells containing the 38 considered eddy covariance sites for each model.

Table S1. List of eddy covariance sites used in this study. Plant functional type (IGBP class), coordinates, and data citation are reported.

Site code	PFT	Latitude	Longitude	Data citation
BE-Bra	MF	51.3092	4.5206	https://doi.org/10.18160/YVBQ-K6WF
BE-Vie	MF	50.3051	5.9981	https://doi.org/10.18160/DF9X-QMRK
CA-Ca3	ENF	49.5346	-124.9004	https://doi.org/10.17190/AMF/1480302
CA-Cbo	DBF	44.3167	-79.9333	https://doi.org/10.17190/AMF/1854365
CA-Gro	MF	48.2167	-82.1556	https://doi.org/10.17190/AMF/1902823
CA-LP1	ENF	55.1119	-122.8414	https://doi.org/10.17190/AMF/1832155
CA-TP4	ENF	42.7102	-80.3574	https://doi.org/10.17190/AMF/1246012
CA-Oas	DBF	53.6289	-106.1978	https://doi.org/10.17190/AMF/1375197
CA-Obs	ENF	53.9872	-105.1178	https://doi.org/10.17190/AMF/1375198
CH-Dav	ENF	46.8153	9.8559	https://doi.org/10.18160/1JA9-VJEV
CH-Lae	MF	47.4781	8.3650	https://doi.org/10.18160/51Z6-S5XF
CZ-BK1	ENF	49.5021	18.5369	https://doi.org/10.18160/2X51-1SD0
CZ-Stn	DBF	49.0360	17.9699	https://doi.org/10.18160/0JY0-ZCD6
DE-Hai	DBF	51.0792	10.4522	https://doi.org/10.18160/CR66-PJ24
DE-Hzd	DBF	50.9638	13.4898	https://doi.org/10.18160/2G60-ZHAK
DE-Obe	ENF	50.7836	13.7196	https://doi.org/10.18140/FLX/1440151
DE-Tha	ENF	50.9636	13.5669	https://doi.org/10.18160/8FBV-1K18
FI-Hyy	ENF	61.8475	24.2950	https://doi.org/10.18160/XTBV-XCJV
FI-Let	ENF	60.6418	23.9595	https://doi.org/10.18140/FLX/1440227
FR-FBn	MF	43.2408	5.6787	https://doi.org/10.18160/KGN6-K1CX
FR-Fon	MF	48.4764	2.7801	https://doi.org/10.18160/X1J0-H684
IL-Yat	ENF	31.3450	35.0520	https://doi.org/10.18160/MAGT-CWRW
IT-Lav	ENF	45.9553	11.2812	https://doi.org/10.18160/HZSQ-G19C
IT-Ren	ENF	46.5869	11.4337	https://doi.org/10.18160/WMCA-8P4P
RU-Fyo	ENF	56.4617	32.9239	https://doi.org/10.18160/XMER-D4NR
US-Bar	DBF	44.0646	-71.2881	https://doi.org/10.17190/AMF/2006969
US-GLE	ENF	41.3665	-106.2399	https://doi.org/10.17190/AMF/1871136

US-Ha1	DBF	42.5378	-72.1715	https://doi.org/10.17190/AMF/1871137
US-Me2	ENF	44.4523	-121.5574	https://doi.org/10.17190/AMF/1854368
US-MMS	DBF	39.3232	-86.4131	https://doi.org/10.17190/AMF/1854369
US-MOz	DBF	38.7441	-92.2000	https://doi.org/10.17190/AMF/1854370
US-NR1	ENF	40.0329	-105.5464	https://doi.org/10.17190/AMF/1871141
US-Oho	DBF	41.5545	-83.8438	https://doi.org/10.17190/AMF/1246089
US-Slt	DBF	39.9138	-74.5960	https://doi.org/10.17190/AMF/1246096
US-SP3	ENF	29.7548	-82.1633	https://doi.org/10.17190/AMF/1246102
US-Uaf	ENF	64.8663	-147.8555	https://doi.org/10.17190/AMF/1480322
US-UMB	DBF	45.5598	-84.7138	https://doi.org/10.17190/AMF/2204882
US-Vcp	ENF	35.8624	-106.5974	https://doi.org/10.17190/AMF/1246122

Table S2. Variables from eddy covariance dataset used in this study.

Variables	**Description**	**Time scale**	**Unit**
NEE_VUT_USTAR50	Net Ecosystem Exchange, using Variable Ustar Threshold (VUT) for each year, from 50 percentile of USTAR threshold, half-hourly data	Half-hourly	umol m^{-2} s^{-1}
GPP_NT_VUT_USTAR50	Gross Primary Production, from Nighttime partitioning method, based on NEE_VUT_USTAR50, calculated from half-hourly data	daily	gC m^{-2} day^{-1}
TA_F_DAY	Averaged daytime air temperature	daily	deg C
VPD_F_MDS	Vapor Pressure Deficit, gapfilled using MDS method, average from half-hourly data	daily	hPa
P_F	Sum of precipitation from half-hourly data	daily	mm day^{-1}
LE_F_MDS	Latent heat flux, gapfilled using MDS method, average from half-hourly data	daily	W m^{-2}
SW_IN_F_MDS	Shortwave radiation, incoming, gapfilled using MDS (negative values set to zero, e.g., negative values from instrumentation noise), average from half-hourly data	daily	W m^{-2}

Table S3. Simulations from TRENDY v9 used in this study.

Simulations	**CO_2 concentration**	**Climate**	**LULCCs forcing**
S0	Pre-industrial	Pre-industrial	Pre-industrial
S1	Observed	Pre-industrial	Pre-industrial
S2	Observed	Observed	Pre-industrial
S3	Observed	Observed	LUH2/HYDE

Supplementary text S1. Testing the statistical method to incorporate the cumulative effect of nitrogen deposition (N_{dep}) to the β estimation

We develop the so-called *GPP residual method* that statistically captures the sensitivity of GPP to CO_2 and climate variables at different time scales to account for co-linearities among the drivers (Methods). We note that the GPP residual may also include other long-term effects specific to individual sites, such as signals related to nitrogen deposition (N_{dep}). Similar to the increasing CO_2 effect, the response to N_{dep} change is likely a long-term phenomenon and might even show some degree of hysteresis, associated with the slow-turnover pools of nitrogen (N) in wood and soil (Gilliam et al., 2019). The input of N_{dep} could be taken up by vegetation and microbes and subsequently redistributed within the plant-soil system, or be retained or stored in the soil or biomass for extended periods before being released or lost through various processes (Galloway et al., 2004). Thus, it's crucial to account for the cumulative effect of N_{dep} that undergoes cycling within the natural system. Assuming a long residence time of reactive nitrogen in the system (Gruber & Galloway, 2008), the accumulated N_{dep} at year t in this analysis can be considered as:

$$Accumulated\ {N_{dep}}_t = \sum_{i=1}^{t} {N_{dep}}_i \qquad (1)$$

Where ${N_{dep}}_i$ is the mean N_{dep} at year i. We also explored applying a low-pass filter to the input data when calculating accumulated N_{dep} at a later stage (Equation 2, 3), to capture the dynamic of N cycling. Our statistical method aims to separate the short-term responses (e.g., temperature, VPD, etc.) from long-term responses (e.g., CO_2). There may be an opportunity to take one more step to further isolate the effects of CO_2 and accumulated N_{dep} from these long-term responses. However, this is challenging as CO_2 and accumulated N_{dep} may be correlated at a long-term scale, which complicates the task of separating these two factors using the linear regression models. We assess the feasibility of integrating accumulated N_{dep} into our *GPP residual method* using both synthetic data and eddy covariance record.

We conduct three sets of tests (Table S4) to integrate the cumulative effect of N_{dep} (η) into the linear regression model of $GPP_{residual}$ after eliminating the climate effect using the GPP residual method (Figure 1d and Methods). Within each set of tests, we employ five linear regression models to examine the influence of co-linearity among independent variables and to determine if the cumulative effect of N_{dep} can be effectively isolated. Specifically, the five linear regression models are designed as: (1) M1: $GPP_{residual} \sim CO_2$. The linear model M1 is used to calculate the CO_2 fertilization effect (β) as the slope in the main text; (2) M2: $GPP_{residual} \sim CO_2 + N_{dep}$ calculates both β and η that are coefficients associated with CO_2 and accumulated N_{dep} (referred to as N_{dep} in the linear models for simplicity), respectively; (3) M3: $GPP_{residual} \sim CO_2$ + years is employed to calculate the coefficient β amidst a linear sequence (here years) within the linear regression model. This is an examination of whether the linear regression model accurately attributes effects when co-linearity among independent variables is anticipated; (4) M4: $GPP_{residual} \sim N_{dep}$ attributes all long-term effects on GPP to accumulated N_{dep} as η. We assess whether accumulated N_{dep}, as the sole independent variable, explains the majority of the variance in $GPP_{residual}$; (5) M5: $GPP_{residual} \sim$ years calculates the trend of $GPP_{residual}$ as the slope. The accumulated N_{dep} (Equation 1) is used in M2 and M4 linear regression models in all three tests.

The distinctions among the three sets of tests lie in the derivation of the $GPP_{residual}$. In **Test #1**, the dependent variable $GPP_{residual}$ is modeled by the terrestrial biosphere model QUINCY, which is used in the main text to develop and evaluate the GPP residual method (Methods). $GPP_{residual}$ is calculated as the difference between simulations forced with transient CO_2 and constant CO_2, reflecting the theoretical comprehension of the CO_2 fertilization effect. Consequently, within the test set, β in M1, M2 and M3 should be comparable if the linear regression models can successfully isolate the CO_2 effect, even with different combinations of independent variables. The R^2 in M4 is expected to be low since no N_{dep} effect is encoded in the QUINCY $GPP_{residual}$.

In **Test #2**, $GPP_{residual}$ is derived from the QUINCY simulation forced with transient CO_2 using the GPP residual method (Methods). Given that the GPP residual method can only separate the short-term climate effect with other long-term effects, the $GPP_{residual}$ may encompass other long-term effects (such as long-term GPP acclimatation to climate) besides the CO_2 effect. These effects are likely to be attributed to CO_2 or other drivers exhibiting a trend by the linear regression model. However, since nitrogen dynamics are not accounted in these simulations, the R^2 in M4 is anticipated to be low.

In **Test #3**, $GPP_{residual}$ is derived from the eddy covariance (EC) dataset using the GPP residual method. Potentially, there could be other long-term effects present in $GPP_{residual}$ aside from CO_2, such as the impact of N_{dep}.

Test #1 and **Test #2** involve 166 synthetic sites in the QUINCY experiments, serving as the proof-of-concept as discussed in the main text. **Test #3** incorporates 38 EC sites used for estimating β and γ, also discussed in the main text.

Table S4. Linear regression models of the $GPP_{residual}$ used to test the cumulative effect of N_{dep} calculated by equation 1

Test #1 $GPP_{residual}$ modeled by QUINCY				
Linear regression models	**Median β ($gC\ m^{-2}\ yr^{-1}\ ppm^{-1}$)**	**Median η ($KgC\ KgN^{-1}$)**	**Median trend ($gC\ m^{-2}\ yr^{-2}$)**	**Mean R^2**
M1: $GPP_{residual} \sim CO_2$	5.78	-	-	0.718
M2: $GPP_{residual} \sim CO_2 + N_{dep}$	4.32	4.55	-	0.727
M3: $GPP_{residual} \sim CO_2$ + years	3.95	-	3.37	0.728
M4: $GPP_{residual} \sim N_{dep}$	-	25.88	-	0.715
M5: $GPP_{residual} \sim$ years	-	-	12.14	0.717
Test #2 $GPP_{residual}$ derived by the *GPP residual method* in QUINCY simulation				
Linear regression models	**Median β ($gC\ m^{-2}\ yr^{-1}\ ppm^{-1}$)**	**Median η ($KgC\ KgN^{-1}$)**	**Median trend ($gC\ m^{-2}\ yr^{-2}$)**	**Mean R^2**
M1: $GPP_{residual} \sim CO_2$	5.82	-	-	0.356
M2: $GPP_{residual} \sim CO_2 + N_{dep}$	3.01	10.40	-	0.368
M3: $GPP_{residual} \sim CO_2$ + years	2.84	-	6.67	0.369
M4: $GPP_{residual} \sim N_{dep}$	-	26.77	-	0.356
M5: $GPP_{residual} \sim$ years	-	-	12.28	0.356
Test #3 $GPP_{residual}$ derived by the *GPP residual method* in EC dataset				
Linear regression models	**Median β ($gC\ m^{-2}\ yr^{-1}\ ppm^{-1}$)**	**Median η ($KgC\ KgN^{-1}$)**	**Median trend ($gC\ m^{-2}\ yr^{-2}$)**	**Mean R^2**
M1: $GPP_{residual} \sim CO_2$	3.18	-	-	0.100
M2: $GPP_{residual} \sim CO_2 + N_{dep}$	-3.33	20.30	-	0.168
M3: $GPP_{residual} \sim CO_2$ + years	-3.69	-	24.23	0.168
M4: $GPP_{residual} \sim N_{dep}$	-	11.77	-	0.145
M5: $GPP_{residual} \sim$ years	-	-	13.85	0.144

We find that the mean R^2 in M1, M4 and M5 are comparable in all three sets of tests (Table S4). That means all predictors, here CO_2, accumulated N_{dep} and years explain an equal proportion of the variance in the $GPP_{residual}$. This implies that either all predictors are equally important, or the collinearity between predictors create redundance in the model. As we priorly know that the $GPP_{residual}$ in **Test #1** is modeled by QUINCY simulations and only include the CO_2 effect, the latter implication is valid. Or in another word, this suggests that the linear regression is likely to misattribute the cumulative N_{dep} effect even when there is no actual influence of N_{dep} on the dependent variable, simply because CO_2 and accumulated N_{dep} exhibit strong correlation, as any other linear sequence (e.g., years). Statistics in **Test #2** show consistency with **Test #1**, where the misattribution to N_{dep} exist when there is no effect of N_{dep} in the $GPP_{residual}$. These findings challenge the linear regression model's capability to effectively handle co-linearity issues. In **Test #3**, the estimation of β by M2 become negative after incorporating accumulated N_{dep} into the linear regression model. While it's possible that the N_{dep} effect influences the relevance of GPP in **Test #3**, the accuracy of the β estimation is likely compromised due to collinearity issues identified in the previous two tests with QUINCY simulations.

As N_{dep} might not have an immediate effect, we adjusted the method of accumulating N_{dep} to assign less importance to N_{dep} in the current time step, while accounting for a higher impact of N_{dep} accumulated in past years. Following this logic, we calculated accumulated N_{dep} to account for the total amount of nitrogen that has been deposited over a specific period (here the window size is set as ten years):

$$Accumulated\ N_{dep_t} = \sum_{i=0}^{9} N_{dep_{t-i}} \times Weight_i \quad (2)$$

Where t denotes year t, and $\mathrm{Weight_i}$ is the weight assigned to the N_{dep} value at time step t-i following the formula:

$$Weight_i = e^{-\alpha\cdot(9-i)} \quad (3)$$

Where α is the decay rate parameter controlling the rate of decay and is set as a constant value of 0.1. i ranges from 0 to 9, representing the past ten time steps within the window. This characteristic of the exponential decay allows for a balance between considering recent values and incorporating historical data in the accumulation process.

Using the same sets of tests as Table S4, but only changing the method of accumulated N_{dep} (Equation 2, 3), the results shown in Table S5 are different.

The low R^2 in M4 in all three tests highlights the inadequacy of solely using accumulated N_{dep} as a predictor to explain the variance of $GPP_{residual}$. However, unlike the η in **Test #1** and **Test #2**, η in **Test #3** shows negative sign (Table S5). This discrepancy can be attributed to the declining trend of N_{dep} near most EC sites (Figure S10a). This decline aligns with reported trends in N_{dep} in Europe and the eastern U.S. (Ackerman et al., 2019; Gilliam et al., 2019; Nopmongcol et al., 2019; Schmitz et al., 2019). The declining trend of annual N_{dep} will also lead to declining accumulated N_{dep} calculated by equations 2 and 3, as they consider the accumulated N_{dep} over the past ten years. It's worth noting that the 166 synthetic sites in QUINCY are randomly distributed across the globe, thus exhibiting both positive and negative trend in N_{dep}.

Although the estimation of β by M2 in **Test #3** decreases after incorporating N_{dep} into the linear regression model (Table S5), the negative sign of η suggests that it is likely a statistical spurious attribution, primarily due to the declining trend in N_{dep}. Experiments show that the positive effect of N addition on productivity persist for a long time even after ceasing the N load (Hrevušová et al., 2009; Meng et al., 2023). The duration for which the benefits of N retention persist after adding it to the ecosystem is closely linked to the balance between N input from biological nitrogen fixation and N_{dep}, and N loss through processes such as leaching and denitrification (Sokolov et al., 2008; Zaehle & Dalmonech, 2011; Davies-Barnard et al., 2020). Uncertainties in the terrestrial N cycling such as the rate of denitrification, pose challenges in understanding the resident time of N, as various factors (e.g., climate, vegetation type, soil texture, pre-disturbance nutrient levels) can influence the processes (Galloway et al., 2004; Sokolov et al., 2008; Davies-Barnard et al., 2020). Given these uncertainties and the scarcity of global data on terrestrial N cycling (Zaehle & Dalmonech, 2011), it is hard to conclude how to integrate N_{dep} to account for the cumulative effect of N_{dep} on vegetation productivity.

Table S5. Linear regression models of the $GPP_{residual}$ used to test the cumulative effect of N_{dep} calculated by equation 2 and 3

Test #1 $GPP_{residual}$ modeled by QUINCY				
Linear regression models	**Median β (gC m^{-2} yr^{-1} ppm^{-1})**	**Median η (KgC KgN^{-1})**	**Median trend (gC m^{-2} yr^{-2})**	**Mean R^2**
M1: $GPP_{residual} \sim CO_2$	5.78	-	-	0.718
M2: $GPP_{residual} \sim CO_2 + N_{dep}$	5.73	-1.40	-	0.724
M3: $GPP_{residual} \sim CO_2$ + years	3.95	-	3.37	0.728
M4: $GPP_{residual} \sim N_{dep}$	-	44.75	-	0.328
M5: $GPP_{residual} \sim$ years	-	-	12.14	0.717
Test #2 $GPP_{residual}$ derived by the *GPP residual method* in QUINCY simulation				
Linear regression models	**Median β (gC m^{-2} yr^{-1} ppm^{-1})**	**Median η (KgC KgN^{-1})**	**Median trend (gC m^{-2} yr^{-2})**	**Mean R^2**
M1: $GPP_{residual} \sim CO_2$	5.81	-	-	0.355
M2: $GPP_{residual} \sim CO_2 + N_{dep}$	5.67	1.25	-	0.366
M3: $GPP_{residual} \sim CO_2$ + years	2.68	-	6.72	0.369
M4: $GPP_{residual} \sim N_{dep}$	-	47.40	-	0.168
M5: $GPP_{residual} \sim$ years	-	-	12.22	0.369
Test #3 $GPP_{residual}$ derived by the *GPP residual method* in EC dataset				
Linear regression models	**Median β (gC m^{-2} yr^{-1} ppm^{-1})**	**Median η (KgC KgN^{-1})**	**Median trend (gC m^{-2} yr^{-2})**	**Mean R^2**
M1: $GPP_{residual} \sim CO_2$	3.18	-	-	0.100
M2: $GPP_{residual} \sim CO_2 + N_{dep}$	2.01	-18.59	-	0.143
M3: $GPP_{residual} \sim CO_2$ + years	-4.07	-	22.24	0.166
M4: $GPP_{residual} \sim N_{dep}$	-	-43.79	-	0.071
M5: $GPP_{residual} \sim$ years	-	-	13.84	0.142

Isolating the long-term effects, including N_{dep} and CO_2, poses great challenge. In our tests, we accumulated N_{dep} using two different methods: i) cumulative way (Equation 1); ii) accumulating by applying an exponential decay with sliding window (Equation 2, 3). The divergent results highlight the importance of future research in selecting appropriate time-scales, and employing causal inference methods to more effectively disentangle the long-term effects on GPP in ecosystems with tightly coupled carbon-nitrogen-climate interactions.

References:

Ackerman, D., Millet, D. B., & Chen, X. (2019). Global Estimates of Inorganic Nitrogen Deposition Across Four Decades. *Global Biogeochemical Cycles*, *33*(1), 100–107. https://doi.org/10.1029/2018GB005990
Davies-Barnard, T., Meyerholt, J., Zaehle, S., Friedlingstein, P., Brovkin, V., Fan, Y., Fisher, R. A., Jones, C. D., Lee, H., Peano, D., Smith, B., Wårlind, D., & Wiltshire, A. J. (2020). Nitrogen cycling in CMIP6 land surface models: Progress and limitations. *Biogeosciences*, *17*(20), 5129–5148. https://doi.org/10.5194/bg-17-5129-2020
Galloway, J. N., Dentener, F. J., Capone, D. G., Boyer, E. W., Howarth, R. W., Seitzinger, S. P., Asner, G. P., Cleveland, C. C., Green, P. A., Holland, E. A., Karl, D. M., Michaels, A. F., Porter, J. H., Townsend, A. R., & Vöosmarty, C. J. (2004). Nitrogen Cycles: Past, Present, and Future. *Biogeochemistry*, *70*(2), 153–226. https://doi.org/10.1007/s10533-004-0370-0
Gilliam, F. S., Burns, D. A., Driscoll, C. T., Frey, S. D., Lovett, G. M., & Watmough, S. A. (2019). Decreased atmospheric nitrogen deposition in eastern North America: Predicted responses of forest ecosystems. *Environmental Pollution*, *244*, 560–574. https://doi.org/10.1016/j.envpol.2018.09.135
Gruber, N., & Galloway, J. N. (2008). An Earth-system perspective of the global nitrogen cycle. *Nature*, *451*(7176), 293–296. https://doi.org/10.1038/nature06592
Hrevušová, Z., Hejcman, M., Pavlů, V. V., Hakl, J., Klaudisová, M., & Mrkvička, J. (2009). Long-term dynamics of biomass production, soil chemical properties and plant species composition of alluvial grassland after the cessation of fertilizer application in the Czech Republic. *Agriculture, Ecosystems & Environment*, *130*(3), 123–130. https://doi.org/10.1016/j.agee.2008.12.008
Meng, Y., Li, T., Liu, H., Li, S., Xu, Z., & Jiang, Y. (2023). Legacy effects of nitrogen deposition and increased precipitation on plant productivity in a semi-arid grassland. *Plant and Soil*, *491*(1), 69–84. https://doi.org/10.1007/s11104-022-05550-x
Nopmongcol, U., Beardsley, R., Kumar, N., Knipping, E., & Yarwood, G. (2019). Changes in United States deposition of nitrogen and sulfur compounds over five decades from 1970 to 2020. *Atmospheric Environment*, *209*, 144–151. https://doi.org/10.1016/j.atmosenv.2019.04.018
Schmitz, A., Sanders, T. G. M., Bolte, A., Bussotti, F., Dirnböck, T., Johnson, J., Peñuelas, J., Pollastrini, M., Prescher, A.-K., Sardans, J., Verstraeten, A., & de Vries, W. (2019). Responses of forest ecosystems in Europe to decreasing nitrogen deposition. *Environmental Pollution*, *244*, 980–994. https://doi.org/10.1016/j.envpol.2018.09.101
Sokolov, A. P., Kicklighter, D. W., Melillo, J. M., Felzer, B. S., Schlosser, C. A., & Cronin, T. W. (2008). Consequences of Considering Carbon–Nitrogen Interactions on the Feedbacks between Climate and the Terrestrial Carbon Cycle. *Journal of Climate*, *21*(15), 3776–3796. https://doi.org/10.1175/2008JCLI2038.1
Zaehle, S., & Dalmonech, D. (2011). Carbon–nitrogen interactions on land at global scales: Current understanding in modelling climate biosphere feedbacks. *Current Opinion in Environmental Sustainability*, *3*(5), 311–320. https://doi.org/10.1016/j.cosust.2011.08.008